Appl. Phys. A 79, 747–751 (2004)
DOI: 10.1007/s00339-004-2567-4

Applied Physics A
Materials Science & Processing

B.S. LUK'YANCHUK ✉
Z.B. WANG
W.D. SONG
M.H. HONG

Particle on surface: 3D-effects in dry laser cleaning*

Data Storage Institute, Agency for Science, Technology and Research, Singapore 117608, Singapore

Received: 27 October 2003/Accepted: 15 December 2003
Published online: 26 July 2004 •

ABSTRACT Previous analysis of dry laser cleaning within the frame of a one-dimensional (1D) model with homogeneous surface heating shows that this model disagrees with experiments by one–two orders of magnitude. The particle on the surface produces an inhomogeneous intensity distribution in its vicinity due to scattering and diffraction. This produces a nonstationary 3D distribution of the temperature and nonstationary 3D thermal deformations of the surface. If one uses the Mie theory for calculation of inhomogeneous intensity then in some region of the parameters, the 3D model predicts results close to the experimental ones. The next step was done when the scattering effects for radiation reflected from the surface was taken into account (so-called "particle on surface" problem). This approach yields results close to the experimental one within the wide range of parameters.

PACS 42.25.Fx; 42.25.Hz; 81.65.Cf

1 Introduction

Theoretical models of dry laser cleaning are based on the idea of fast thermal expansion of the particle and/or substrate [1, 2]. There are two types of models typically used: 1) the so-called one-dimensional (1D) model, where it was assumed that the presence of the particle only weakly changes the distribution of intensity [3–7], and 2) the so-called three-dimensional (3D) model, which takes into account the effect of intensity inhomogeneity [8–12]. 1D model provides correct qualitative understanding of the main peculiarities of dry laser cleaning but often yields big (1–2 orders of magnitude) disagreement with experimental values of the cleaning threshold. The reason for this discrepancy is related to the scattering of radiation by contaminant particle, which strongly changes the local distribution of absorbed laser intensity. We analyzed some characteristic features related to 3D effects, using the Mie theory for calculation of the intensity distribution [13]. This model predicts results close to the experimental ones in some intermediate region of particle sizes. Nevertheless for "small" and for "big" particles, it produces deviations from the experimental threshold, although smaller then within 1D model (see Fig. 9 in [13]). One can discuss this situation as a failure of both, 1D and 3D thermal expansion models. For example, authors of [14] consider that for Si substrate "dry laser cleaning" is, in fact, everywhere the "ablative cleaning", i.e., momentum transfer to the particle arises not due to the thermal expansion, but due to evaporation of substrate under the particle. This ablative cleaning mechanism certainly exists [11, 15], but previously authors considered it a particular mechanism for some range of parameters. In the given paper we present the results of calculations with the 3D model, where we consider that the Mie theory is insufficient for examination of the intensity distribution and the scattering effects for radiation reflected from the surface was taken into account (the so-called "particle on surface" problem [8, 16]). We show that this approach yields agreement with the experiment within the wide range of parameters.

2 Light focusing and near-field enhancement

As it was shown in [8–13], the particle significantly changes the local intensity distribution. There are two easily understandable limiting cases: the geometrical optics limit, when the size of the particle (radius a) is significantly larger than the radiation wavelength, $a \gg \lambda$. For this case the intensity on the substrate can be estimated using ray tracing according to Snell's law and energy conservation [13, 17]. This approach yields intensity enhancement factor [17]:

$$\frac{I_{\mathrm{m}}}{I_0} \approx \frac{a^2}{w_{\mathrm{g}}^2} \approx \frac{27n^4}{(4-n^2)^3}, \tag{1}$$

where n is refractive index of the particle.

Another useful limit follows from the dipole approximation for small spheres, $a \ll \lambda$, which yields the simple approximation for optical enhancement given by [17]

$$\frac{I_{\mathrm{m}}}{I_0} \approx \left(1+\frac{n^2-1}{n^2+2}q^2\right)^2. \tag{2}$$

Here $q = 2\pi a/\lambda$ is the size parameter. Comparison of (1) and (2) shows that for a refractive index $1.1 < n < 1.7$ transition to the geometrical optics limit occurs for the size parameter around $3.5 < q < 5.5$. In the paper [17] the smooth interpolation formula (transfer from the dipole approximation to

✉ Fax: +65/6777 1349,E-mail:boris_lukiyanchuk@dsi.a-star.edu.sg
*Plenary lecture on the 3rd International Workshop on Laser Cleaning (Crete, Greece, October 3–4, 2003)

geometrical optics) was suggested. Although it qualitatively explains the role of the particle size effect, the situation is more complex because of the structure of the field within the caustic cone. For spherical particles, this structure was discussed under approximation of the Mie theory in [13]. Similar results also follow for cylindrical symmetry [18]. It should be noted that even for the big size parameter (limit of geometrical optics) exact solution of the Maxwell equations yields a complex pattern, related to caustic diffraction catastrophes [19]. A well-known example is the Airy pattern [20], which is discussed due to its relation to super-resolution near field structure [21]. Another example is the cusp diffraction catastrophe presented by Pearcey function [19, 22, 23]

$$\Psi(x,z)=\frac{1}{\sqrt{2\pi}}\int\limits_{-\infty}^{\infty}\mathrm{d}s\ \exp\left[\mathrm{i}\left(\frac{s^4}{4}+\frac{s^2}{2}z+sx\right)\right], \tag{3}$$

Here Ψ is a complex function of two normalized variables, while intensity is considered to be $I\propto|\Psi|^2$. The path of integration in (3) is such that the integrand vanishes at its terminal points. The intensity distribution, presented by the Pearcey function [19, 22] is qualitatively similar to those, which follow from the solution of the wave equation for the cylinder [18] (Fig. 1a). The peculiarity of the diffraction pattern for the spherical particle is an additional caustic line along the z-axis [13] (Fig. 1b). This caustic is responsible for the maximal laser intensity under the particle. The prediction of geometrical optics [24] is valid within the caustic cone, but *not* on the z-axis.

The distribution of the z-component of the Poynting vector under the particle in x–y-plane can be quite often with sufficient accuracy approximated by a Gaussian function [13]:

$$S(x,y)=S_0\,\mathrm{e}^{-r^2/r_0^2}, \tag{4}$$

where r is radial coordinate and S_0 is the intensity enhancement factor. Distributions of the intensity (from the Mie theory) have different widths along the x and y directions (see in Fig. 5a), nevertheless we approximate the total field by a Gaussian function with $r_0=\sqrt{x_0y_0}$. Values S_0 and r_0 oscillate versus size parameter due to optical resonance effect, see in Figs. 5 and 6 in [13]. Typical values of the field enhancement for 1 μm PS particle and radiation with $\lambda=248$ nm are $S_0\approx10^2$ and $r_0\approx50$ nm. Within the intensity distribution one can clearly see three regions: enhanced field, shadow and homogeneous intensity [11, 13]. In many cases this distribution can be approximated by sum of three Gaussian distributions [13]:

$$I(r,t)=I_0(t)\left[1+S_0\,\mathrm{e}^{-r^2/r_0^2}-S_1\,\mathrm{e}^{-r^2/r_{\mathrm{sh}}^2}\right]. \tag{5}$$

This approximation consists of three parts: 1) out of particle at $r>r_{\mathrm{sh}}\approx a+\lambda$ it tends to homogeneous 1D intensity I_0; 2) in the region of enhanced radiation at $r<r_0$ it tends to enhanced field intensity S_0I_0; 3) in the region of "shadow", $r_0<r<r_{\mathrm{sh}}$, intensity is rather small. The surface intensity is understood as z-component of the Poynting vector.

3 Particle on surface

The "particle on surface" problem has the exact solution given by [16]. We applied this solution for a laser cleaning problem in [8]. Practical usage of this solution needs, however, a long calculation time, related to the calculation of Weyl type integrals within the matrix, which describes reflection of the spherical wave:

$$\Pi_\ell^{\mathrm{m}}(r)=\frac{\mathrm{i}^{-\ell}}{2\pi}\int\limits_0^{2\pi}\mathrm{d}\beta\int\limits_0^{\pi/2-\mathrm{i}\infty}\mathrm{d}\alpha\sin\alpha\mathrm{e}^{\mathrm{i}kr\cos\gamma}Y_\ell^{\mathrm{m}}(\alpha,\beta)\,, \tag{6}$$

where $Y_\ell^{\mathrm{m}}(\alpha,\beta)$ are the spherical harmonics, related to associated Legendre polynomials. Working on this paper we have prepared the FORTRAN program, which permits us to do calculations in a reasonable time.

In spite of difficulties with the numerical calculations, the situation is rather clear from the physical point of view. Qualitatively the substrate surface works like a mirror coupled with spherical resonator (particle); it should lead to an increase in optical enhancement S_0 and a decrease in the area of the field localization r_0 (sharpening effect). This effect is confirmed by calculations. In Fig. 2 the intensity distribution within the

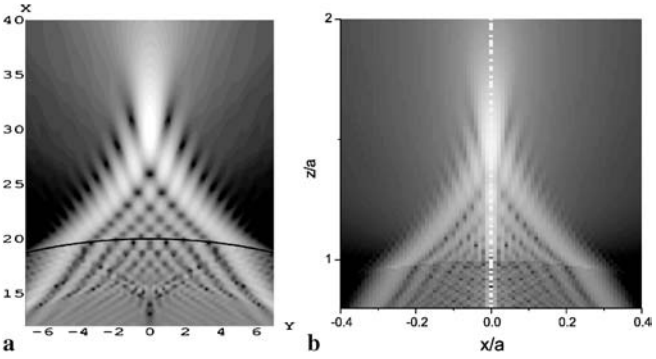

FIGURE 1 Distribution of the intensity within the caustic of the particle with the refractive index $n=\sqrt{2}$ and the radius of $a=30\lambda$. At the limit of geometrical optics $n=\sqrt{2}$ corresponds to the situation when rays are focused exactly into the backside of the particle. **a** Diffraction pattern for cylindrical symmetry (see details in [18]); **b** diffraction pattern for spherical particle, calculated by the Mie theory

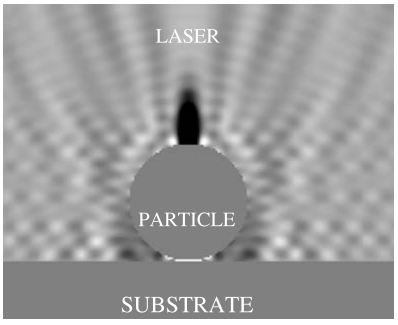

FIGURE 2 The intensity $I=S_z$ distribution within the x–z plane for radiation with $\lambda=248$ nm, scattered by a polystyrene particle ($n=1.6$, $a=0.5$ μm) on Si surface. Gradations of the intensity are given from negative (*dark*) to positive (*light*) values. *Dark area* on the *top* of the particle corresponds to energy flux directed up, while *white area* under the particle corresponds to the energy flux directed to the substrate

xz plane is shown; one can see enhanced radiation intensity, which came through the transparent particle after its reflection by surface. This effect may play a role for enhanced Raman scattering.

The presence of the surface may qualitatively influence intensity distribution. For example, two peak intensity distribution, which follows under approximation of the Mie theory, can be at some conditions converted into a single peak distribution within the particle on surface problem. This effect arises due to strong variation of the field enhancement factor from the center of the particle onto the particle periphery. This effect was demonstrated experimentally in [15] and was confirmed by calculations with the help of Multiple Multipole (MMP) technique. In this paper [15] the authors discussed the intensity of radiation as $I = |E|^2$. Our calculations for the z-component of the Poynting vector, which are shown in Fig. 3, confirm the discussed in [15] effect.

In Fig. 4 we present the field enhancement factor and effective widths of the intensity distribution for polysterene particles on silicon surface. Comparing this picture with previous results, which follow from the Mie theory (see e.g., Figs. 5, 6 in [13]) one can see a more complex picture for the optical resonance effect vs size parameters.

The reflection of radiation from the surface and its secondary scattering produces a smoother distribution of the intensity (compare to Mie theory) on the surface of substrate within the main lobe, see e.g., in Fig. 5. At the same time far from this lobe, the distribution of intensity becomes more complex, see in Fig. 6. Additional oscillations in the intensity distribution are produced by interference of scattered and reflected radiation, similar to Newton rings.

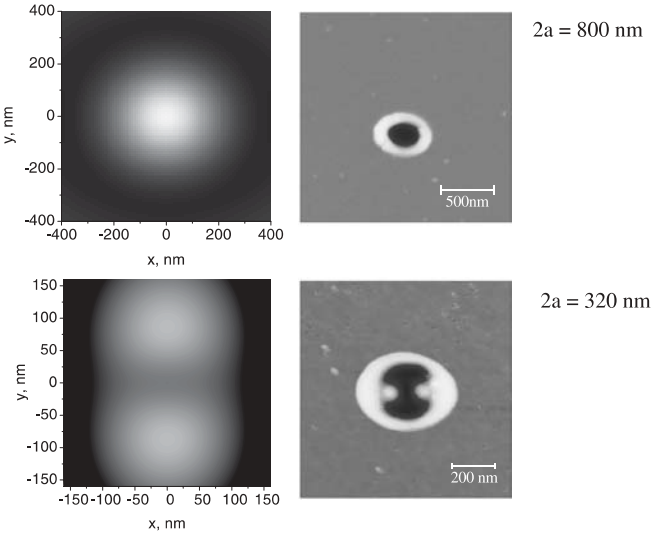

FIGURE 3 *Left pictures* presents contour plots for the intensity distribution ($\lambda = 800$ nm) under the spherical particle with size $2a = 800$ nm (single peak) and $2a = 320$ nm (two peaks). Calculations were done for the polystyrene (PS) particle on Si surface. The electrical field was considered to be oriented in vertical direction. The *right AFM pictures* are results of experiments [15], where the corresponding pattern was developed by illumination of a Ti-Sapphire fs laser pulse. The modified surface is "photo" of the intensity distribution on the surface of Si. *Left pictures* are in a good agreement with experiment. For example, the size of the optically enhanced region is about 400 nm for $2a = 800$ nm particle and distribution has a single peak. For a particle with $2a = 320$ nm size, the distribution of intensity has two peaks with spacing between peaks at about 200 nm

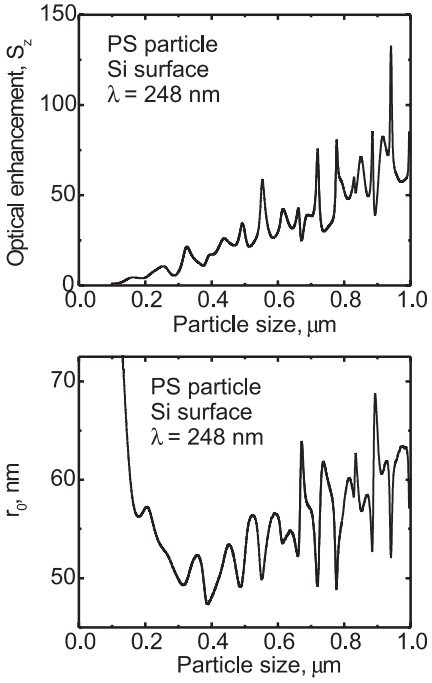

FIGURE 4 *(top)* Field enhancement factor, S_0 vs. particle size calculated for the polystyrene particle with refractive index $n = 1.6$ ($\lambda = 248$ nm). *(bottom)* Width of the intensity distribution, $r_0 = \sqrt{x_0 y_0}$ versus particle size

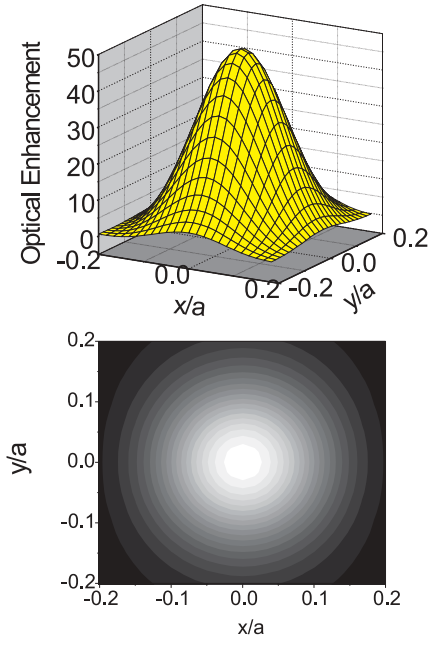

FIGURE 5 Field enhancement factor, S_0 calculated for 1 μm SiO_2 particle on Si surface for radiation with $\lambda = 248$ nm. *Bottom plot* shows topography of this distribution

Further steps in calculations are the same as in [13]. Having distribution (5) we calculate the temperature distribution from the heat equation, considering the smooth laser pulse with pulse duration 23 ns. This temperature distribution is used to solve the 3D thermal deformation problem. The value of the thermal deformation is used to solve the problem of the particle dynamics in adhesion potential. We use the same cri-

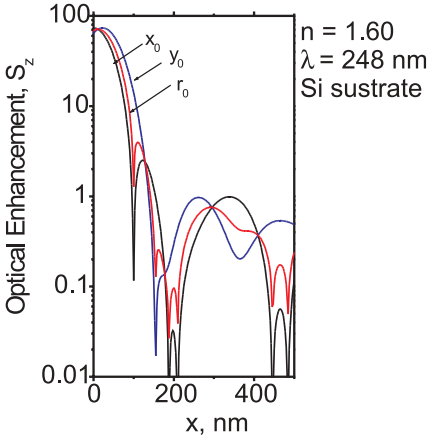

FIGURE 6 Distribution of the field enhancement factor S_z along x and y axes and the averaged distribution for polystyrene particle $n = 1.6$ ($\lambda = 248$ nm) with size $2a = 1$ μm on Si substrate

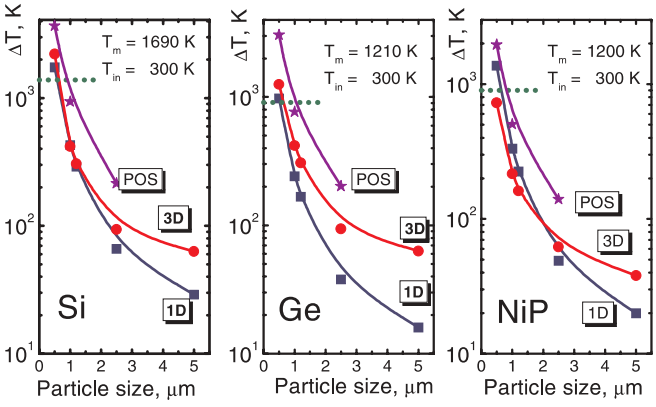

FIGURE 7 Theoretical (for 1D and 3D + 1D models) and the experimental results of the threshold laser fluences for SiO_2 particles on Si, Ge and NiP substrates. Excimer laser 248 nm, pulse duration 23 ns. *Bottom curves* are calculated from the particle on surface theory

terium for the particle removal as in [13]. The final result of the calculations is presented in Fig. 7. One can see from the figure that intensity distribution given by "particle on surface" yield threshold fluence which is significantly closer to the experimental results compared to the case when this distribution is taken from the Mie theory. It is interesting to note that the "plunging" of the particles into the substrate due to plastic deformations [25] yields a variation of the particle "effective permittivity". It is a well known effect in the theory of island films [26]. "Plunging" of the PS particle into the Si surface (at $\lambda = 248$ nm) yields an increase of effective permittivity of the PS particle. One can roughly estimate this increase with the help of Lorentz–Lorenz formula [26].

The last result, presented in Fig. 8, shows the calculated temperature under the particle at threshold fluence. One can see that this temperature is higher then corresponding temperature, calculated with the intensity distribution from the Mie theory. From these calculations follows that the region of "ablative cleaning" mechanism for small particle increases, as well as the region of the "splashing cleaning" mechanism (splash of melt yields the particle removal). Nevertheless it follows from our model that thermal expansion of dry laser cleaning mechanism is still valid for sufficiently big particles. In any case, this problem should

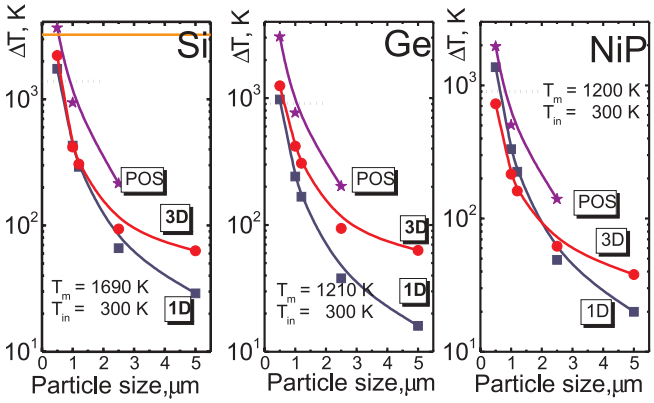

FIGURE 8 Maximal surface temperature (for 1D and 3D models) at threshold fluences, which were presented in Fig. 7. POS-calculations from "particle on surface" problem

be clarified experimentally e.g., with the help of optical pirometry.

4 Conclusion

This paper continues our previous examination [13] of 3D effects in dry laser cleaning. The basic point is that instead of the Mie theory, we have used the exact solution of the "particle on surface" problem. The presented model takes into account the field enhancement effect, 3D thermal elasticity effects and the true temporal pulse shape. The cleaning threshold found from this model for the particles with sizes from 0.5 to 2.5 μm is significantly closer to the experiment as compared to the 3D model which uses approximation of the Mie theory.

ACKNOWLEDGEMENTS We are very thankful to Prof. S. Anisimov, Prof. D. Bäuerle and Dr. N. Arnold for discussions. Part of this work was done under support of Russian Foundation for Basic Research (grants 01-02-16136 and 01-02-16189).

REFERENCES

1 D. Bäuerle: *Laser Processing and Chemistry*, 3rd edn. (Springer Verlag, Berlin 2000)
2 B.S. Luk'yanchuk (Ed.): *Laser Cleaning* (Word Scientific, New Jersey, London 2002)
3 J.D. Kelley, F.E. Hovis: Microelectron. Eng. **20**, 159 (1993)
4 Y.F. Lu, W.D. Song, B.W. Ang, M.H. Hong, S.S.H. Chan, T.S. Low: Appl. Phys. A **65**, 9 (1997)
5 Y.F. Lu, Y.W. Zheng, W.D. Song: J. Appl. Phys. **87**, 1534 (2000)
6 N. Arnold, G. Schrems, T. Mühlberger, M. Bertsch, M. Mosbacher, P. Leiderer, D. Bäuerle: Proc. SPIE **4426**, 340 (2002)
7 N. Arnold: In Ref. [2], Chapt. 2, pp. 51–102
8 B.S. Luk'yanchuk, Y.W. Zheng, Y.F. Lu: Proc. SPIE **4065**, 576 (2000)
9 B.S. Luk'yanchuk, Y.W. Zheng, Y.F. Lu: Proc. SPIE **4423**, 115 (2001)
10 B.S. Luk'yanchuk, Y.W. Zheng, Y.F. Lu: RIKEN Rev. **43**, 28 (2002)
11 B.S. Luk'yanchuk, M. Mosbacher, Y.W. Zheng, H.-J. Münzer, S.M. Huang, M. Bertsch, W.D. Song, Z.B. Wang, Y.F. Lu, O. Dubbers, J. Boneberg, P. Leiderer, M.H. Hong, T.C. Chong: In Ref. [2], Chapt. 3, pp. 103–178
12 B.S. Luk'yanchuk, S.M. Huang, M.H. Hong: Proc. SPIE **4760**, 204 (2002)
13 B.S. Luk'yanchuk, N. Arnold, S.M. Huang, Z.B. Wang, M.H. Hong: Appl. Phys. A **77**, 209 (2003)
14 N. Arnold, G. Schrems, D. Bäuerle: Ablative threshold in laser cleaning of particles, Abstract of 7th Int. Conf. on Laser Ablation, COLA 03 (Crete, Greece 2002)

15 H.-J. Münzer, M. Mosbacher, M. Bertsch, O. Dubbers, F. Burnmeister, A. Park, R. Wannemather, B.-U. Runge, D. Bäuerle, J. Boneberg, P. Leiderer: Proc. SPIE **4426**, 180 (2002)
16 P.A. Bobbert, J. Vlieger: Physica A **137**, 209 (1986)
17 N. Arnold: Appl. Surf. Sci. **208–209**, 15 (2003)
18 W. Zalowich: Phys. Rev. E, **64**, 066610 (2001)
19 M.V. Berry, C. Upstill: In *Progress in optics*, Vol. 18, ed. by E. Wolf, (Elsevier, North-Holland 1980)
20 M. Born, E. Wolf: *Principles of Optics*, 7th edn. (Cambridge University Press, 1999)
21 T.R.M. Sales: Phys. Rev. Lett. **81**, 3844 (1998)
22 J.F. Nye: J. Opt. A: Pure Appl. Opt. **5**, 495 (2003)
23 T. Miyamoto: Nonlinear Anal. **54**, 755 (2003)
24 Yu.A. Kravtsov, Yu.I. Orlov: *Geometrical Optics of Inhomogeneous Media* (Springer, Berlin 1990)
25 G. Schrems, M.P. Delamare, N. Arnold, P. Leiderer, D. Bäuerle: Appl. Phys. A **76**, 847 (2003)
26 D. Bedeaux, J. Vlieger: *Optical Properties of Surface* (Imperial College Press, London 2002)